J. Phys. B: At. Mol. Opt. Phys. 25 (1992) 4507-4517. Printed in the UK

Multiphoton ionization of Rb_2 in the wavelength range 620–670 nm

Hidetoshi Suemitsu†, Hideki Kitaura†, Ryoichiro Yokoyama†, Masahiro Ehara‡ and Hiroshi Nakatsuji‡

† Department of Engineering Science, Faculty of Engineering, Kyoto University, Kyoto 606, Japan
‡ Department of Synthetic Chemistry, Faculty of Engineering, Kyoto University, Kyoto 606, Japan

Received 27 May 1992, in final form 29 July 1992

Abstract. The relative production rates of Rb^+ and Rb_2^+ ions through the multiphoton ionization (MPI) of Rb_2 and the effective order of non-linearity k for these ions were measured in the wavelength range 620-670 nm. The measured results indicated that these ions were produced by two- or three-photon ionization of Rb_2. The Franck-Condon factors calculated for the transition from the ground state ($X\,^1\Sigma_g^+$) to the first intermediate state ($B\,^1\Pi_u$) were in good agreement with the production rates obtained for Rb^+ and Rb_2^+ ions. From these reasons we concluded that in the process of MPI of Rb_2 the transition to the $B\,^1\Pi_u$ state plays a crucial role in the production of both ions.

The competitive relations between the production processes of Rb_2^+ and Rb^+ ions were derived. In the wavelength range at around 669 nm the ratio of the number of Rb^+ ions to that of Rb_2^+ ions produced through three-photon ionization of Rb_2 was about 4/1. Supposing this ratio is constant over a whole wavelength range, it was estimated that in 638-658 nm the production process of Rb_2^+ through two-photon ionization occupied 90-95% of all MPI processes.

1. Introduction

When a focused CW laser with wavelength range 620-670 nm is directed through rubidium vapour, Rb_2^+ and Rb^+ ions are formed. The Rb atom does not have any excited state which can resonate with one incident photon in this wavelength range. In this case it is known that very high power laser (about 10^{8-10} W cm^{-2}) is necessary to produce an Rb^+ ion by multiphoton ionization (MPI) of the Rb atom (Morellec *et al* 1980). Therefore in a low power laser (400 W cm^{-2}) (the present case), Rb^+ ions are not produced by MPI of Rb atoms. Rb^+ ions are produced by MPI of Rb_2 molecules. However, because the number of rubidium dimers Rb_2 involved in the vapour is about 0.25% of the number of rubidium atoms Rb at 473 K, the probability of MPI for Rb_2 is many orders of magnitude larger than that of Rb. Furthermore it is natural that we think that Rb_2^+ ions are produced by MPI of Rb_2, as well. The ion spectra observed are highly structured. To make clear the relation between the mechanisms by which these ions are produced and the source of this structure is one of the purposes of this paper.

The following processes are thought of as the production processes of Rb_2^+ and Rb^+ ions through MPI of rubidium dimers Rb_2,

$$Rb_2 + 2h\nu \rightarrow Rb_2^{**} \qquad Rb_2^{**} \rightarrow Rb_2^+ + e^- \qquad \text{(autoionization)} \tag{1}$$

$$Rb_2 + 2h\nu \rightarrow Rb_2^{*} \qquad Rb_2^{*} + h\nu \rightarrow Rb_2^+ + e^- \tag{2}$$

$$Rb_2 + 2h\nu \rightarrow Rb_2^{**} \qquad Rb_2^{**} + h\nu \rightarrow Rb_2^+ + e^- \tag{2'}$$

$$Rb_2 + 2h\nu \rightarrow Rb_2^{*} \qquad Rb_2^{*} + h\nu \rightarrow Rb^+ + Rb + e^- \tag{3}$$

$$Rb_2 + 2h\nu \rightarrow Rb_2^{**} \qquad Rb_2^{**} + h\nu \rightarrow Rb^+ + Rb + e^- \tag{3'}$$

where Rb_2^{**} is the super excited state of the Rb_2 molecule. The super excited states are defined as the excited states of Rb_2 which exist in the energy region above the ionization limit of Rb_2. The Rydberg states with the large principal quantum number which converge to the ground state $1^2\Sigma_g^+$ of Rb_2^+ have rovibronic states in the energy region over the ionization limit. These rovibronic states are the super excited states. The super excited states also involve many of the two-electron excited states of the Rb_2 molecule. Rb_2^* are Rydberg states which have large principal quantum numbers and also converge to $1^2\Sigma_g^+$ of Rb_2^+, but these rovibronic states are in the energy region below the ionization limit.

For the understanding of the production processes and the relative production rates of Rb^+ and Rb_2^+ ions, we need to know the exact values of the potential energy and the molecular constants for the ground and excited states of Rb_2 and Rb_2^+. In particular,

Table 1. Computed and experimental spectroscopic constants of Rb_2 and Rb_2^+ states.

State	R_e (Å)	T_e (cm^{-1})	D_e (eV)	ω_e (cm^{-1})	Reference
Rb_2: X $^1\Sigma_g^+$	4.075		0.512	54.90	Th: Spiegelmann *et al* (1989)
	4.19		0.480	57.0	Th: Igel-mann *et al* (1986)
	4.2099		0.494	57.780	Exp: Amiot *et al* (1985)
				57.747	Exp: Caldwell *et al* (1980)
			0.488		Exp: Breford and Engelke (1980)
				57.7743	Exp: Kotnik-Karuza and Vidal (1979)
			0.480	57.45	Exp: Tsi-Ze and San-Tsiang (1937)
				57.31	Exp: Kusch (1936)
				57.8	Exp: Matuyama (1934)
B $^1\Pi_u$	4.430	14 969		46.92	Th: Spiegelmann *et al* (1989)
		14 665.447		47.316	Exp: Caldwell *et al* (1980)
		14 665.537		47.387	Exp: Kotnik-Karuza and Vidal (1979)
		14 662.6		48.05	Exp: Kusch (1936)
		14 666		47.3	Exp: Matuyama (1934)
Rb_2^+: $1^2\Sigma_g^+$			0.75–0.1		Exp: Wagner and Isenor (1985)
			0.76		Exp: Von Szentpaly *et al* (1982)
			0.72–0.06		Exp: Klucharev *et al* (1980)
			0.79		Th: Schwartmann (1979)
	4.5		0.66		Th: Valance (1978)
	3.96		0.67		Th: Valance (1976)
			0.80–0.85		Exp: Borodin *et al* (1975)
	4.44		0.862		Th: Bellmonte *et al* (1974)
			0.73–0.06		Th: Beckel and Engelke (1972)
			0.73		Exp: Lee and Mahan (1965)
			0.80		Th: Von Preuss (1955)

exact knowledge of the ground state and the first intermediate state B $^1\Pi_u$ is necessary. Spiegelmann *et al* (1989) gave reliable potential curves for these two levels by *ab initio* calculations. Their value for the potential minimum (T_e) of B $^1\Pi_u$ was about 300 cm^{-1} higher than the values determined by many other experimenters. Also D_e values of the ground states X $^1\Sigma_g^+$ of Rb_2 and $1^2\Sigma_g^+$ of the Rb_2^+ ion are important to determine the ionization potential of Rb_2 and there are many theoretical and experimental values reported by many researchers. In table 1 these values are shown together with other molecular constants.

In this paper, we attempt to explain the experimental results of the relative production rates from calculations based on a few assumptions. We estimate the production processes of Rb_2^+ and Rb^+ ions through MPI of Rb_2. Furthermore we analyse the competitive relation between the production processes of Rb_2^+ and Rb^+ ions and determine the ratios of the number of ions produced through these processes from the experimental results.

2. Experimental

A detailed description of the apparatus used has already been given in previous papers (Suemitsu *et al* 1990, 1991, 1992). For convenience, a brief sketch is given in figure 1. A CW ring dye laser (Coherent, Model CR699) combined with an Ar^+ ion laser (Coherent, Model I-100-18) was orthogonally crossed with the Rb beam. DCM was used as dye, which covered the wavelength range 620–670 nm. The laser power was kept at 350 mW in the whole wavelength range during the experiment. The focused laser beam showed a Gaussian distribution with a diameter of 0.24 mm as the full width at half maximum (FWHM). The laser was confirmed to be in a single mode and to have about 20 MHz as FWHM by spectral analyser. The Rb beam was initially produced by the oven which was kept at 483 K and was introduced into the ionization region through the small hole of the partition. It is expected that in this region the Rb beam is geometrically expanded to a cross sectional diameter of about 15 mm. We suppose that the ratio of Rb_2 molecules to Rb atoms in the beam is the same as that in the oven. Since the mean free path of Rb in the oven at this temperature is much

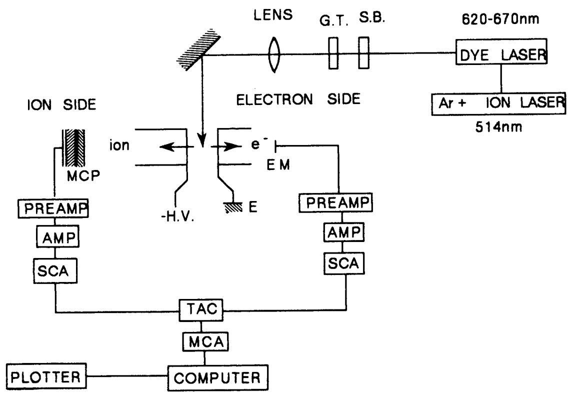

Figure 1. Schematic diagram of the experimental set-up. G.T.: Glan–Thompson Prism, S.B.: Soleil–Babine compensator, E.M.: electron multiplier, MCP: microchannel plate, TAC: time to amplitude converter, MCA: multichannel analyser.

larger than the size of the exit hole of the oven, the Rb beam is considered as a molecular flow. The Rb_2^+ and Rb^+ ions produced are mass-analysed by the time-of-flight method.

Figure 2 shows the relative production rates of Rb_2^+ and Rb^+ ions produced through MPI of Rb_2 in the wavelength range 620–670 nm. That for the Rb_2^+ ion has a threshold at about 635 nm, a broad peak at about 655 nm and becomes almost constant over 665 nm. The yield has many structures on the main curve. On the other hand, that for the Rb^+ ion has a threshold at about 635 nm and increases gradually with an increase in wavelength. That does not indicate any broad peak in the range 630–670 nm, but indicates many structures over this wavelength range.

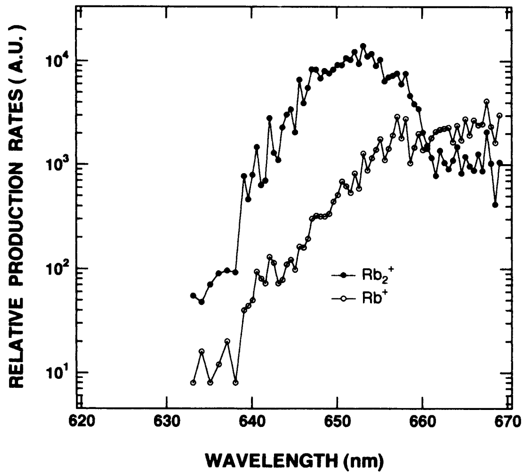

Figure 2. The relative production rates of Rb_2^+ and Rb^+ ions produced through the multiphoton ionization of Rb_2 as a function of wavelength.

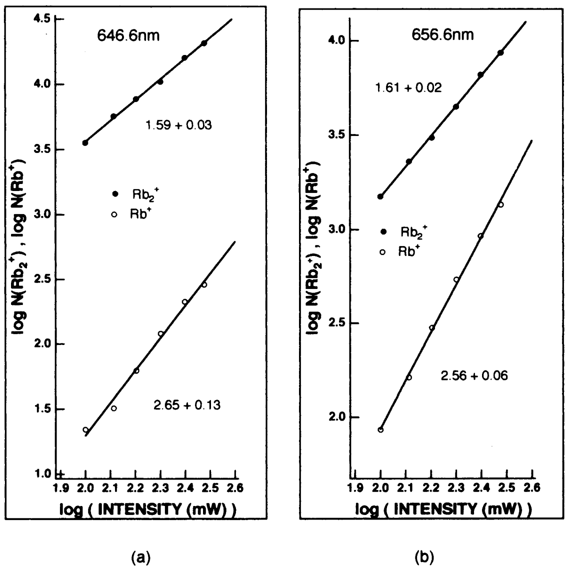

Figure 3. Typical examples of $\log(N(Rb_2^+))$ and $\log(N(Rb^+))$ against log(intensity(mW)) for two wavelengths. The slopes show the effective order of non-linearity k. $N(Rb_2^+)$ and $N(Rb^+)$ are the number of Rb_2^+ and Rb^+ ions produced, respectively.

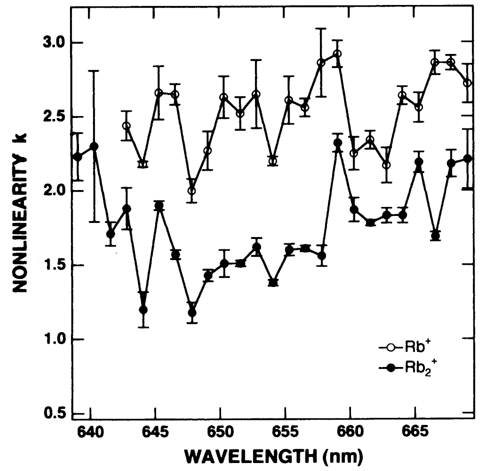

Figure 4. Effective order of non-linearity k of Rb_2^+ and Rb^+ ions as a function of wavelength.

Figure 3 shows the count number of Rb_2^+ and Rb^+ ions as a function of laser intensity at two wavelengths. The full lines were drawn by the root mean square fitting method. These slopes show the effective order of non-linearity k. In figure 4 the values of k for Rb^+ and Rb_2^+ ions are given as a function of the wavelength. The value of k indicates the minimum number of photons which participate in the photoionization. We need three photons to produce Rb^+ ions through MPI of Rb_2 and two or three photons for Rb_2^+ ions. The values of k for the Rb^+ ion are between 2 and 3 in the range 640–670 nm. On the other hand, the values of k for the Rb_2^+ ion repeatedly 'go up and down' between 1 and 2 and exceed 2 with an increase in wavelength.

3. Calculations

In figure 5 we show the potential curves for several states of Rb_2 and Rb_2^+ that are closely connected with MPI of Rb_2. In this figure we used the molecular constants obtained experimentally by Wagner and Isenor (1985), Caldwell *et al* (1980) and Amiot *et al* (1985) in drawing the potential curves for $1^2\Sigma_g^+$ (Rb_2^+ ion), B $^1\Pi_u$ and X $^1\Sigma_g^+$ (Rb_2), respectively. In the first glance at this figure we should notice that the Rb^+ ions are produced only by three-photon ionization of the rubidium dimers Rb_2, and the Rb_2^+ ions are produced by two- or three-photon ionization of the rubidium dimers Rb_2. The number of Rb^+ ions produced through three-photon ionization is proportional to the three-photon ionization cross sections σ of Rb_2. The cross sections σ are given by

$$\sigma \propto \sum_{v''} e^{-E_{v''}/kT} \left| \sum_{i,j} \frac{\mu_{v''i}\mu_{ij}\mu_{j2}}{\Delta\omega_i \Delta\omega_j} \right|^2 \tag{4}$$

where $E_{v''}$ is the energy of the vibrational level v'' of the ground state X $^1\Sigma_g^+$, k and T are the Boltzmann factor and the temperature of the oven, respectively, μ_{lm} are the transition dipole moments coupling with the initial and final states through the intermediate states, and $\Delta\omega_i$ and $\Delta\omega_j$ are $(E_{v'} - E_{v''}) - E_p$ and $(E_v - E_{v''}) - 2E_p$, respectively. $E_{v'}$, E_v and E_p are the energy of the vibrational levels of the first, second intermediate states and the incident photon, respectively.

Generally the sum in equation (4) will be dominated by the term with the largest intermediate state coupling, i.e., small $\Delta\omega_i$ or $\Delta\omega_j$. However, when more than one

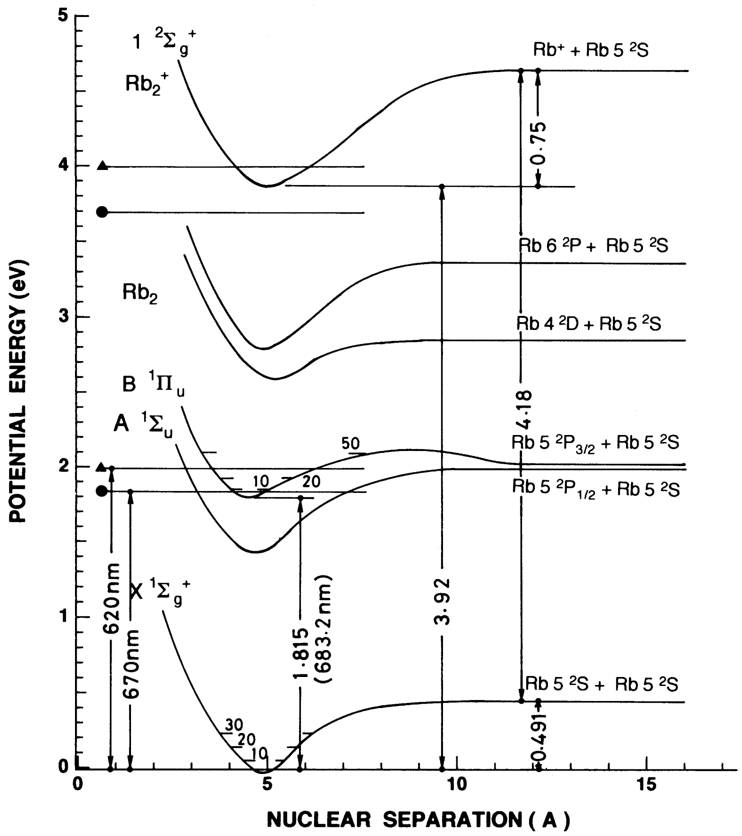

Figure 5. Potential curves of the ground and the few excited states of Rb_2 and Rb_2^+ ions.

intermediate state contributes significantly to the three-photon ionization cross section, interference effects will modulate the size of the cross section. To simplify the calculation, we ignore these interference effects by replacing equation (4) with the modified expression

$$\sigma \propto \sum_{v''} e^{-E_{v''}/kT} \sum_{i,j} \frac{|\mu_{v_i''}|^2 |\mu_{ij}|^2 |\mu_{j2}|^2}{\Delta\omega_i^2 \Delta\omega_j^2}. \tag{5}$$

In equation (5) $|\mu_{ij}|^2$, $|\mu_{j2}|^2$ and $|\Delta\omega_j|^2$ will be less dependent on the incident photon energy, because the second intermediate states j consist of the rovibronic levels of many Rydberg states with high principal quantum number and overlap each other, and we can consider these states to be quasicontinuum ones. This will be true for the final states 2, too. Furthermore if $|\Delta\omega_i|^2$ satisfies the resonance condition and γ is the linewidth, equation (5) will be replaced by

$$\sigma \propto \sum_{v''} e^{-E_{v''}/kT} \sum_{i} |\mu_{v''i}|^2 \frac{\gamma}{\Delta\omega_i^2 + \gamma^2}. \tag{6}$$

If the electronic part in $|\mu_{v''i}|^2$, that is, $|d_{0i}|^2$ is constant and the FCF are weak functions of the rotational quantum number, equation (6) is reduced as follows,

$$\sigma \propto a \sum_{v''} e^{-E_{v''}/kT} \sum_{i} |\langle v''|v_i'\rangle|^2 \frac{\gamma}{\Delta\omega_i^2 + \gamma^2} \tag{7}$$

$$\sigma \propto \sum_{v''} e^{-E_{v''}/kT} \sum_i |\langle v''|v_i'\rangle|^2 \frac{\gamma}{\Delta\omega_i^2 + \gamma^2} \tag{8}$$

where $a = |d_{0i}|^2 = \text{const}$.

Using the potential energy curves of the ground state X $^1\Sigma_g^+$ and the intermediate states B $^1\Pi_u$ which were calculated by Spiegelmann *et al* (1989), calculating the FCF as $\gamma = 3\ \text{cm}^{-1}$, and summing over v'' of 0 to 20 and over v_i' of 0 to 50, we obtain (*a*) in figure 6. This curve agrees very well with the experimental results for the Rb^+ ion, except for the difference of 14 nm in the wavelength. This difference of the wavelength at the threshold will mainly originate in the fact that the minimum of the potential energy (T_e) of the B $^1\Pi_u$ state calculated by Spiegelmann *et al* (1989) is by about $300\ \text{cm}^{-1}$ larger in magnitude than that obtained experimentally. When we make a parallel translation of the potential curve for the B $^1\Pi_u$ state by $303\ \text{cm}^{-1}$ in magnitude and calculate equation (8), the results become as shown in figure 6(*b*). Though the results are still different by about 10 nm from the experimental results in the wavelength of the threshold, a good improvement was recognized. However, the origin of this remaining difference is not apparent yet.

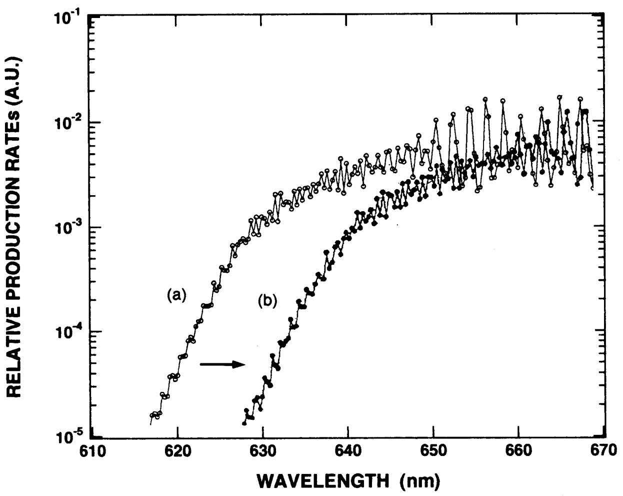

Figure 6. The calculated relative production rates of the Rb^+ ion produced through three-photon ionization of Rb_2. (*a*) The results calculated using the original potential curves given by Spiegelmann *et al* (1989) for the ground state X $^1\Sigma_g^+$ and the intermediate states B $^1\Pi_u$. (*b*) The results calculated using the potential curve shifted down by $303\ \text{cm}^{-1}$ parallel to the original one for B $^1\Pi_u$.

4. Discussion

Rb_2^+ ions are not produced only by three-photon ionization, but also by two-photon ionization. When two times the energy of the incident photon plus $E_{v''}$, that is, $2h\nu + E_{v''}$ exceeds the ionization potential I_p of Rb_2, Rb_2^+ ions are produced through the process (1). However, all of the super excited state Rb_2^{**} produced by the absorption of two photons do not change to Rb_2^+ ions through the autoionization. A part of Rb_2^{**} is ionized to produce Rb^+ and Rb_2^+ ions through the processes (2′) and (3′), respectively. The process (1) competes with the processes (2′) and (3′). The production processes of Rb^+ and Rb_2^+ ions through the three-photon ionization of Rb_2 are competitive processes, too. Let $N_3(Rb^+)$ and $N_3(Rb_2^+)$ represent the number of Rb^+ and Rb_2^+ ions produced through the three-photon ionization of Rb_2, respectively. The ratio of the number of these ions, that is, $N_3(Rb^+)/N_3(Rb_2^+)$, was about 4/1 in the wavelength range around 669 nm, as shown in figure 7. In this wavelength range the rubidium dimers Rb_2 will be ionized only through three-photon ionization. First we suppose that this ratio is constant over the whole wavelength range. Furthermore we suppose that all of Rb_2^{**} produced through the absorption of two photons by the rubidium dimers Rb_2 are ionized by the processes (1), (2′) and (3′). If Q is the rate of Rb_2^+ ions produced by the process (1), Q is given by

$$\begin{aligned} Q &= N_2(Rb_2^+)/\{N_2(Rb_2^+)+(N_3(Rb^+)+N_3(Rb_2^+))\} \\ &= 4*N_2(Rb_2^+)/(5*N_3(Rb^+)+4*N_2(Rb_2^+)) \end{aligned} \tag{9}$$

where $N_2(Rb_2^+)$ is the count number of Rb_2^+ ions produced only by two-photon ionization and $N_3(Rb_2^+)/N_3(Rb^+)=1/4$ was assumed. The rates Q estimated from the present experimental results are shown in figure 8. These results indicate that in the wavelength range 638–654 nm, 90–95% of the rubidium dimers Rb_2 excited to the super excited states Rb_2^{**} are autoionized to produce Rb_2^+ ions. In the wavelength range longer than 654 nm, the number of rubidium dimers Rb_2 excited to the super excited states Rb_2^{**} decreases gradually with an increase in wavelength. Rb^+ ions produced by the process (3) exceed those produced by the competitive process (3′) and finally all Rb^+ ions will be produced by the process (3). Therefore, as is evident from the definition of Q, in the wavelength range longer than 654 nm, the values of Q lose their primary meaning as the rate of competition. In figure 8 we show the rates Q' in the case where $N_3(Rb^+)/N_3(Rb_2^+)$ is 7/3, too. There is no significant difference between the two Q values in 638–654 nm.

On the basis of the above estimated results, we attempt to calculate the photoionization yield for the Rb_2^+ ion. In the case of the two-photon ionization the two-photon

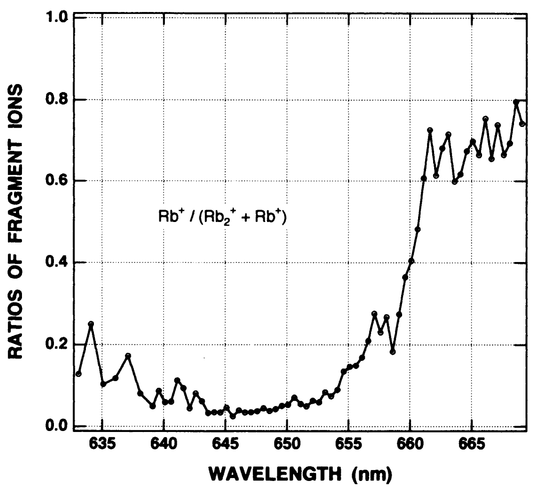

Figure 7. The ratios of the fragment ions produced by the multiphoton ionization of rubidium dimers Rb_2. $N_3(Rb^+)/(N_2(Rb_2^+)+N_3(Rb_2^+)+N_3(Rb^+))$.

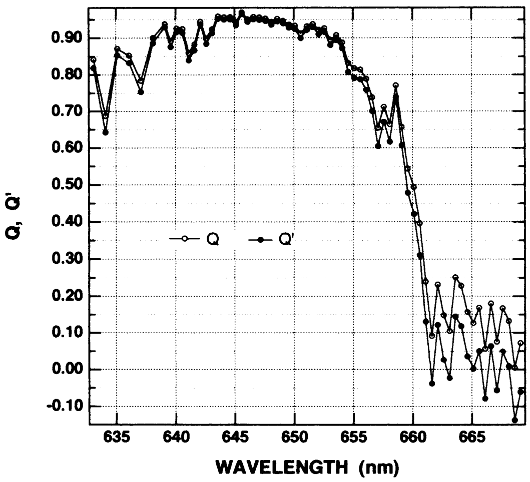

Figure 8. The rates Q and Q' of the number of Rb_2^+ ions produced via the autoionization from the super excited states Rb_2^{**} to the number of Rb^+ ions produced by the participation of one more photon from Rb_2^{**}: Q: $N_3(Rb^+):N_3(Rb_2^+)=8:2$. Q': $N_3(Rb^+):N_3(Rb_2^+)=7:3$.

ionization cross section σ will be given by equation (8), too. The only difference is in the summing methods. When we take the summation of the FCF for v'', we multiply by 9.25 and 0.25 the FCF corresponding to the cases of $E_{v''}+2E_p \geqslant I_p$ and $E_{v''}+2E_p < I_p$, respectively. At this time we supposed $Q=0.9$ and $N_3(Rb^+)/N_3(Rb_2^+)=4/1$. These results are shown in figure 9. The calculated results agree well with the experimental results, except for the slight shift to the short wavelength side.

In the case of the non-resonant multiphoton ionization, the effective order of the non-linearity k indicates definitely how many photons participate in this process. However, in the case of the alkali dimers things are much more complicated. In this case the initial states are populated in the vibrational levels with the Boltzmann

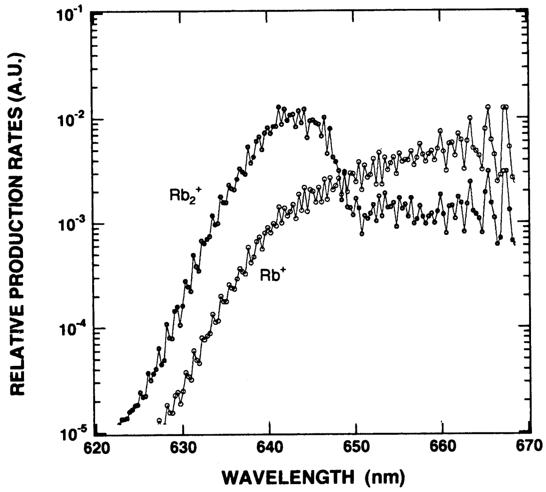

Figure 9. The calculated relative production rates of Rb_2^+ and Rb^+ ions using $Q=0.9$ and $N_3(Rb^+)/N_3(Rb_2^+)=4/1$, which values were obtained from figures 6 and 7.

distribution decided at the present temperature (at 473 K, 48% of the rubidium dimers are initially in the vibrational ground state) and in summing up FCF over $v''=0$–20 we have to multiply each FCF by the Boltzmann factor as the weight. This has an effect upon the values of k and will obscure their values. As shown in figure 4, the values of k for the Rb^+ and Rb_2^+ ions are between 2 and 3 and between 1 and 2, respectively. Both k are roughly similar in the spectral pattern. In particular, k for Rb_2^+ becomes larger and larger with an increase in wavelength and finally exceeds 2. This indicates that the production processes of the Rb_2^+ ion are gradually shifting from the process (1) to the process (2) with an increase in wavelength. On the other hand, k for the Rb^+ ion is between 2 and 3 over the whole wavelength range of 643–670 nm. These experimental results indicate that the Rb^+ ions are produced through the processes (3) and (3′).

5. Conclusions

The relative production rates of Rb_2^+ and Rb^+ ions through two- or three-photon ionization of the rubidium dimers Rb_2 were measured in the wavelength range 620–670 nm. The effective order of non-linearity k was measured in the range 643–670 nm, as well. From these experimental results we concluded for the production processes of Rb_2^+ and Rb^+ ions as follows.

(1) Most of Rb_2^+ ions are produced through the process (1) in the wavelength range shorter than about 650 nm.

(2) In 650–661 nm the production processes of Rb_2^+ are gradually shifted from the process (1) to the process (2).

(3) Most of the Rb_2^+ ions are produced through the process (3) in the wavelength range longer than 661 nm.

(4) Rb^+ ions are produced through the processes (3) and (3′).

There exist two kinds of competitive processes in the five proposed production processes of Rb_2^+ and Rb^+ ions. One is between the processes ((2) or (2′)) and ((3) or (3′)), which correspond to three-photon ionization processes. The other one is the competitive processes between the processes (1) and ((2′)+(3′)). We conclude that in the former competitive processes the process (3) or (3′) occupies about 80% of three-photon ionization processes and the remaining 20% belongs to the process (2) or (2′). We also conclude that in the latter processes 90–95% of the super excited states Rb_2^{**} is autoionized to produce Rb_2^+ ions through the process (1) and 5–10% of them produce Rb^+ ions through the process (3′).

The overall spectra of the photoionization yield for Rb_2^+ and Rb^+ ions are approximately decided by the FCF from the ground states to the first intermediate states of Rb_2, and thus the second intermediate states and the final states give little effect on the spectra of these ions.

Photoelectric spectroscopy will be the most effective method to make clear what the contribution of each channel is. We are now preparing to do this.

Acknowledgments

This research was done with the support and collaboration of the research group on the WT-III tokamak, Department of Physics, Kyoto University. The authors are indebted to all members of this group for their help. Furthermore the authors thank Professor T Fujimoto for a useful suggestion in carrying out this research. The DIAVIB code developed by Dr N Sato (Keio University) was used for the calculation of FCF.

References

Amiot C, Crozet P and Verges J 1985 *Chem. Phys. Lett.* **121** 390
Beckel C L and Engelke R 1972 *J. Mol. Spectrosc.* **42** 578
Bellomonte L, Cavaliere P and Ferrante G 1974 *J. Chem. Phys.* **61** 3225
Borodin V M, Klyucharev A N and Sepman V Yu 1975 *Opt. Spectrosc.* **39** 231
Breford E J and Engelke F 1980 *Chem. Phys. Lett.* **75** 132
Caldwell C D, Engelke F and Hage H 1980 *Chem. Phys.* **54** 21
Igel-Mann G, Wedig U, Fuentealba P and Stoll H 1986 *J. Chem. Phys.* **84** 5007
Klucharev A N, Lazarenko A V and Vujnovic V 1980 *J. Phys. B: At. Mol. Phys.* **13** 1143
Kotnik-Karuza D and Vidal C R 1979 *Chem. Phys.* **40** 25
Kusch P 1936 *Phys. Rev.* **49** 218
Lee Y T and Mahan B H 1965 *J. Chem. Phys.* **42** 2893
Matuyama E 1934 *Nature* 567
Morellec J, Normand D, Mainfray G and Manus C 1980 *Phys. Rev. Lett.* **44** 1394
Schwartmann W 1979 *PhD thesis* Bochum
Spiegelmann F, Pavolini D and Daudey J P 1989 *J. Phys. B: At. Mol. Opt. Phys.* **22** 2465
Suemitsu H, Imai S, Yoshida E, Imanishi H and Naba I 1990 *J. Phys. Soc. Japan* **59** 1981
Suemitsu H, Imanishi H and Kato H 1992 *J. Phys. Soc. Japan* **61** 1926
Suemitsu H, Yoshida E and Imanishi H 1991 *J. Phys. Soc. Japan* **60** 2907
Tsi-Ze N and San-Tsiang T 1937 *Phys. Rev.* **52** 91
Valance A 1976 *Phys. Lett.* **59A** 271
—— 1978 *J. Chem. Phys.* **69** 355
Von Preuss H 1955 *Z. Naturf.* A **10** 365
Von Szentpaly L, Fuentealba P, Preuss H and Stoll H 1982 *Chem. Phys. Lett.* **93** 555
Wagner G S and Isenor N R 1985 *Can. J. Phys.* **63** 976